ISSN 0949-8257, Volume 15, Number 6

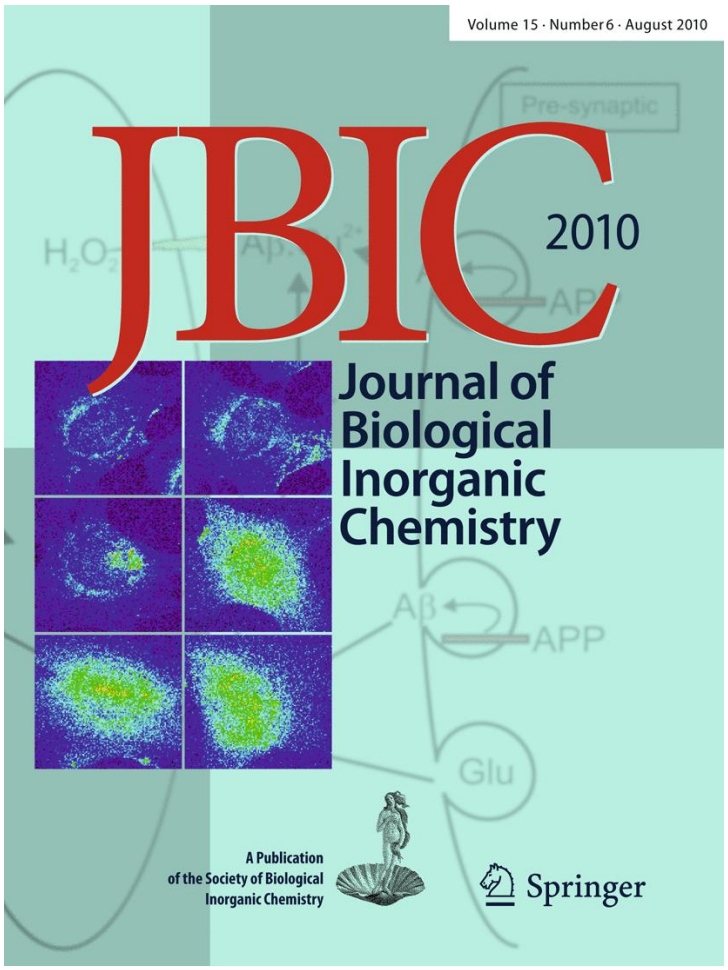

J Biol Inorg Chem (2010) 15:841–850
DOI 10.1007/s00775-010-0648-8

ORIGINAL PAPER

Biological activity of enantiomeric complexes $[PtCl_2L_2]$ (L_2 is aromatic bisphosphanes and aromatic diamines)

Sophie Bombard · Marzia Bruna Gariboldi · Elena Monti · Elisabetta Gabano · Luca Gaviglio · Mauro Ravera · Domenico Osella

Received: 20 January 2010 / Accepted: 9 March 2010 / Published online: 24 March 2010

Abstract Enantiomeric complexes of formula $[PtCl_2L_2]$ [L_2 is (*R*)-(+)-BINAP and (*S*)-(−)-BINAP, where BINAP is 2,2′-bis(diphenylphosphane)-1,1′-binaphthyl, and (*R*)-(+)-DABN and (*S*)-(−)-DABN, where DABN is 1,1′-binaphthyl-2,2′-diamine], were tested for their cytotoxic activity against three cancer cell lines and for their ability to bind to the human telomeric sequence folded in the G-quadruplex structure. Similar experiments were carried out on prototypal complexes cisplatin and *cis*-$[PtCl_2(PPh_3)_2]$ for comparison. Platinum complexes containing phosphanes proved less cytotoxic to cancer cell lines and less likely to interact with the nucleobases of the G-quadruplex than those containing amines; in both cases the *S*-(−) isomer was more active than the *R*-(+) counterpart. More specifically, whereas all the platinum complexes were able to platinate the G-quadruplex structure from the human telomeric repeat, the extent and sites of platination depended on the nature of the ligands. Complexes containing (bulky) phosphanes interacted only with the adenines of the loops, whereas those containing the less sterically demanding amines interacted with adenines and some guanines of the G-quartet.

Keywords Platinum complexes · Phosphanes and amines · DNA quadruplex · Telomere · Cytotoxicity

Electronic supplementary material The online version of this article (doi:10.1007/s00775-010-0648-8) contains supplementary material, which is available to authorized users.

S. Bombard
Laboratoire de Chimie et Biochimie Pharmacologiques et Toxicologiques, CNRS UMR8601,
Université Paris Descartes,
45 Rue des Saints-Pères,
75006 Paris, France

S. Bombard
Laboratoire de l'Homéostasie Cellulaire et Cancer,
INSERM UMR-S1007,
Université Paris Descartes,
45 Rue des Saints-Pères, 75006 Paris, France

M. B. Gariboldi · E. Monti
Dipartimento di Biologia Strutturale e Funzionale,
Università dell'Insubria,
Via A. da Giussano 10, 21052 Busto Arsizio (VA), Italy

E. Gabano · L. Gaviglio · M. Ravera · D. Osella (✉)
Dipartimento di Scienze dell'Ambiente e della Vita,
Università del Piemonte Orientale "Amedeo Avogadro",
Viale T. Michel 11, 15121 Alessandria, Italy
e-mail: domenico.osella@mfn.unipmn.it

Introduction

Today, more than four decades after the serendipitous discovery of its antitumor activity [1, 2], the metallodrug cisplatin has earned a key place in the systemic treatment of cancers, especially in polychemotherapeutic regimes [3]. However, its severe side effects and possible failure in subsequent treatment owing to drug resistance have resulted in a concerted effort to develop new platinum complexes with improved pharmacological properties. To this aim, thousands of analogues have been synthesized (by varying the carrier and/or leaving groups) and tested, but only about 35 compounds have entered clinical trials so far. Carboplatin and oxaliplatin are in routine clinical use worldwide, whereas nedaplatin, lobaplatin, and heptaplatin have achieved regional approval only in Japan, China, and South Korea, respectively [4].

Structure–activity relationship studies by Cleare and Hoeschele [5–7] have demonstrated that effective platinum-based cytotoxic agents should possess a square-planar Pt(II) structure with two chlorides or carboxylates as

leaving groups and two amines as carrier ligands in *cis* configuration. Another variant would consist of phospanes rather than amines.

The chemistry of platinum–phosphane compounds is probably one of the most intensely studied chemistries in inorganic chemistry [8]; the number and diversity of phosphanes synthesized has increased rapidly since the 1960s for the preparation of new and ever-more-efficient homogeneous catalysts [9].

The in vivo antitumor activity of the PPh_3 analogue of cisplatin, namely, *cis*-[$PtCl_2(PPh_3)_2$], and of a series of similar platinum–phosphane complexes has been studied against lymphoid leukemia in mice, but with disappointing results (i.e., median survival time $T/C < 125\%$) [10]. A number of factors may have contributed to this poor outcome: (1) tertiary phosphanes were generally used in aqueous media owing to the easy hydrolysis of P–H bonds; however, the presence of the N–H linkage has been shown to be crucial for the formation of cytotoxic adducts by establishing hydrogen bonds between cisplatin-like complexes and the DNA phosphate backbone; (2) the low water solubility of substituted phosphanes unfavorably affects drug administration and biodistribution; (3) the steric hindrance and *trans*-labilizing effect of substituted phosphanes is higher than that of amines and may cause decreased stability of the Pt–G adducts in DNA. The poor antitumor activity of the phosphane-containing complexes initially studied [10] probably discouraged further research into the biological applications of these compounds.

The aim of the present work was to compare the performance of a panel of platinum-containing complexes (Fig. 1) of the general formula [$PtCl_2L_2$] containing large, chiral, aromatic ligands [L_2 is (*R*)-(+)-BINAP, **1R**, and (*S*)-(−)-BINAP, **1S**, where BINAP is 2,2′-bis(diphenylphosphane)-1,1′-binaphthyl), (*R*)-(+)-DABN, **2R**, and (*S*)-(−)-DABN, **2S**, where DABN is 1,1′-binaphthyl-2,2′-diamine] in terms of their ability to bind DNA nucleobases and to elicit biological effects.

Two parameters were considered in assessing the biological activity of the complexes: their ability to bind to G-quadruplexes in telomeres and to cross-link them, and their overall cytotoxicity on selected human tumor cell lines, namely, A2780 ovarian carcinoma and its cisplatin-resistant form A2780Cp8 and colon adenocarcinoma HCT116. It is well known that the cytotoxic activity of Pt(II) complexes is mainly due to their ability to coordinatively link nuclear DNA.

Telomeres are specialized repeats of G-rich DNA sequences (TTAGGG, in humans) that cap the end of linear eukaryotic chromosomes and prevent their degradation [11]. In normal cells, telomeres shorten by 50–200 bp for each round of replication because of the incomplete end replication of DNA [12]. A limit of telomere length is then reached and the cells undergo senescence and/or apoptosis.

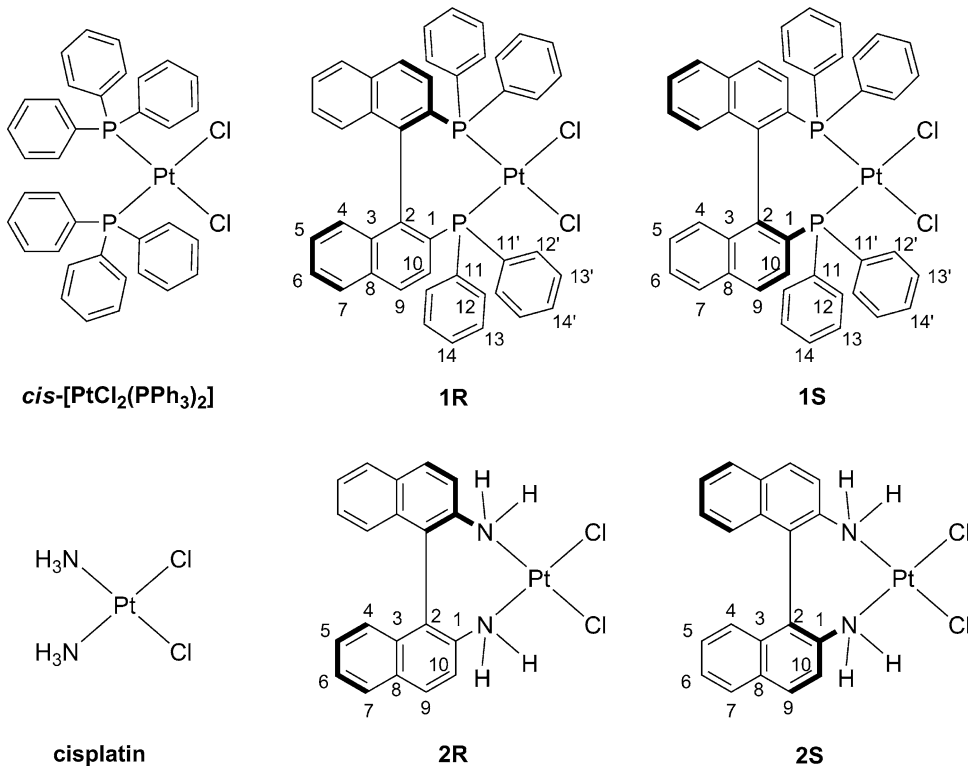

Fig. 1 Structure of the complexes under investigation, with the general formula [$PtCl_2L_2$]: L_2 is 2 × NH_3, cisplatin; 2 × PPh_3, *cis*-[$PtCl_2(PPh_3)_2$]; (*R*)-(+)-BINAP, **1R**; (*S*)-(−)-BINAP, **1S**; (*R*)-(+)-DABN, **2R**, and (*S*)-(−)-DABN, **2S**, where BINAP is 2,2′-bis(diphenylphosphane)-1,1′-binaphthyl and DABN is 1,1′-binaphthyl-2,2′-diamine

Telomerase (the enzyme involved in maintaining telomere length) is usually inactivated in differentiated cells, but it is reactivated in approximately 85–90% of human tumors. It adds telomeric DNA repeats at the 3′ ends of telomeres, compensating for the loss of telomeres at each round of replication and thus contributing to the malignant transformation [13].

The G-rich 3′ extremity of telomeres protrudes as a single strand of about 200 bases. In the presence of monovalent cations, this extremity has been shown to fold, in vitro, into four-stranded DNA structures, called G-quadruplexes, which consist of stacks of G-quartets (four guanines linked by Hoogsteen hydrogen bonds) [11, 14, 15]. Since telomerase requires an unfolded single-stranded substrate, G-quadruplex conformations hinder telomerase activity. Therefore, any compound that stabilizes these G-quadruplexes could conceivably be effective as a telomerase inhibitor and, consequently, as an antitumor agent [16, 17]. It has also been shown that G-quadruplex stabilizers can deprotect telomeres by preventing the binding of essential telomeric proteins; this leads to cellular death, independently of telomerase inhibition [18]. The G-rich telomeres represent an ideal target for platinum complexes [19, 20]. Indeed, the telomere length regulation and telomerase-inhibiting properties of cisplatin and its congeners have already been studied [21–27].

Redon et al. [28, 29] and Ourliac-Garnier et al. [30, 31] demonstrated the ability of G-quadruplex structures to form platinum adducts. Mono- and bifunctional platinum complexes were shown to bind free adenines (preferentially A7 and A19) in the loop regions. Unexpectedly, these complexes also proved to bind the four guanines of one external G-quartet of the antiparallel G-quadruplex structure of the human telomeric sequence (G2, G10, G14, G22), suggesting a transient disruption of the hydrogen bonds of this G-quartet. Such cross-linking would prevent the unfolding of the G-quadruplex, and, hence, inhibit telomerase activity. In contrast, Heringova et al. [32] hypothesized that the binding of cisplatin to its usual N7-G DNA binding site might interfere with the Hoogsteen hydrogen bonding that stabilizes G-quadruplexes; this would either inhibit quadruplex formation or destabilize the quadruplex structure.

A platinum–quinacridine-based compound was found to interact with DNA quadruplexes via a dual mechanism: nucleobase coordination by the electrophilic platinum moiety and π–π interaction (stacking) between the large planar aromatic system and the G-quartet on the external surface of the G-quadruplex [33, 34]. Because they contain aromatic ligands, complexes **1R**, **1S**, **2R**, and **2S** might also act via this dual mechanism.

Materials and methods

Reagents

All chemicals, including cisplatin and *cis*-$[PtCl_2(PPh_3)_2]$ (Aldrich), were of analytical grade and used without further purification. Milli-Q-grade water (18 MΩ cm) was used for the preparation of aqueous solutions.

Physical measurements

Elemental analyses for all the compounds were performed routinely in our laboratories and the experimental values corresponded to within ±0.4% of calculated values.

The NMR spectra were measured with a JEOL Eclipse Plus spectrometer operating at 400 MHz (^{1}H), 100.5 MHz (^{13}C), and 85.9 MHz (^{195}Pt). ^{1}H NMR and ^{13}C NMR chemical shifts were reported in parts per million referenced to residual solvent proton resonances. ^{195}Pt NMR spectra were recorded in $CDCl_3$ or *N,N*-dimethylformamide-d_7 (DMF-d_7), using a solution of $K_2[PtCl_4]$ in aqueous KCl as the external reference. The shift for $K_2[PtCl_4]$ was adjusted to −1,628 ppm with respect to $Na_2[PtCl_6]$ ($\delta = 0$ ppm).

Electrospray mass spectra were obtained using a Micromass ZMD mass spectrometer. Typically, a dilute solution of compound in 0.1:99.9 DMF/methanol or CH_3CN was delivered directly to the spectrometer source at 0.01 mL min^{-1}, using a Hamilton microsyringe controlled by a single-syringe infusion pump. The nebulizer tip operated at 3,000–3,500 V and 150 °C, with nitrogen used both as a drying and as a nebulizing gas. The cone voltage was 30 V for the characterization of the complexes and 15 V for the study of the aquation reactions. Quasimolecular ion peaks $[M+H]^+$ and peaks of sodiated species $[M+Na]^+$ were assigned on the basis of the *m*/*z* values and of the simulated isotope distribution patterns.

Rotatory power measurements were performed with a JASCO P-2000 equipped with an intelligent remote module (6940-J033A), a Peltier temperature controller (PTC-203), and a tungsten–halogen lamp at 589 nm. The measurements were carried out at 25 °C with 2% solutions of DABN ligands and complexes in tetrahydrofuran (THF), and of BINAP ligands and complexes in CH_2Cl_2. Conductivity measurements were performed using an Orion 120 conductivity meter in dimethyl sulfoxide (DMSO) at 25 and 37 ± 0.1 °C using a thermostatic circulating bath to keep the temperature of the sample constant. The analyses were carried out on freshly prepared solutions of the complexes in DMSO (1 mM) by measuring the molar conductivity at regular time intervals. The UV–vis spectra

were recorded in the wavelength range from 200 to 800 nm with a JASCO V550 UV–vis spectrophotometer equipped with a deuterium lamp and a halogen lamp.

Synthesis of platinum complexes **1R**, **1S**, **2R**, and **2S**

*Synthesis of **1R***

Complex **1R** was synthesized according to published procedures [35–37]. ^{1}H NMR ($CDCl_3$): 7.80 (4H, m, H_{12}), 7.60 (4H, br, H_{12}'), 7.56 (2H, d, $^{3}J = 8.06$ Hz, H_4 or H_7), 7.50 (2H, d, $^{3}J = 8.79$ Hz, H_9), 7.40–7.44 (6H, m, $H_{13} + H_{14}$), 7.33–7.37 (4H, m, $H_{10} + H_5$ or H_6), 7.11 (2H, m, H_5 or H_6), 6.82 (2H, m, H_{14}'), 6.74 (2H, d, $^{3}J = 8.06$ Hz, H_4 or H_7), 6.66 (4H, m, H_{13}') ppm; ^{13}C NMR ($CDCl_3$): 138.76 (C_2 or C_3), 135.59 (C_{12}), 134.82 (C_{12}'), 133.88 (C_2 or C_3), 133.06 (C_8), 130.43 (C_{14}'), 131.05 (C_{14}), 129.06 (C_9), 128.14 (C_5 or C_6), 128.05 (C_{10}), 127.71 (C_4 or C_7), 127.62 (C_4 or C_7), 127.54 (C_{13}), 127.31 (C_{13}'), 126.67 (C_5 or C_6), 122.41–121.69 (C_{11}, C_{11}', C_1) ppm; ^{31}P{^{1}H} NMR ($CDCl_3$): 10.50 ppm (satellite bands at −0.86 and 21.81 ppm, $J_{PPt} = 3{,}670$ Hz); ^{195}Pt NMR ($CDCl_3$): −4,223 (t, $J_{PPt} = 3{,}670$ Hz) ppm. Electrospray ionization mass spectrometry (ESI–MS) (CH_3CN): 852.13 (88.88%), 853.13 (100%), 854.13 (58.70%), 855.13 (45.34%), 856.13 (16.99%) calcd for $C_{44}H_{32}ClP_2Pt$; found: 852.18 (89.00%), 853.20 (100%), 854.32 (58.52%), 855.30 (45.27%), 856.13 (17.15%) $[M–Cl]^+$. $[\alpha]_D^{25}$ (CH_2Cl_2): +383° (ligand: +124°).

*Synthesis of **1S***

Complex **1S** was synthesized according to published procedures [35–37]. ^{1}H NMR ($CDCl_3$): 7.80 (4H, m, H_{12}), 7.60 (4H, br, H_{12}'), 7.56 (2H, d, $^{3}J = 8.06$ Hz, H_4 or H_7), 7.50 (2H, d, $^{3}J = 8.79$ Hz, H_9), 7.40-7.44 (6H, m, $H_{13} + H_{14}$), 7.33–7.37 (4H, m, $H_{10} + H_5$ or H_6), 7.11 (2H, m, H_5 or H_6), 6.82 (2H, m, H_{14}'), 6.74 (2H, d, $^{3}J = 8.06$ Hz, H_4 or H_7), 6.66 (4H, m, H_{13}') ppm; ^{13}C NMR ($CDCl_3$): 138.76 (C_2 or C_3), 135.59 (C_{12}), 134.82 (C_{12}'), 133.88 (C_2 or C_3), 133.06 (C_8), 130.43 (C_{14}'), 131.05 (C_{14}), 129.06 (C_9), 128.14 (C_5 or C_6), 128.05 (C_{10}), 127.71 (C_4 or C_7), 127.62 (C_4 or C_7), 127.54 (C_{13}), 127.31 (C_{13}'), 126.67 (C_5 or C_6), 122.41–121.69 (C_{11}, C_{11}', C_1) ppm; ^{31}P{^{1}H} NMR ($CDCl_3$): 10.50 ppm (satellite bands at −0.86 and 21.81 ppm, $J_{PPt} = 3{,}670$ Hz); ^{195}Pt NMR ($CDCl_3$): −4,223 (t, $J_{PPt} = 3{,}670$ Hz) ppm. ESI–MS (CH_3CN): 852.13 (88.88%), 853.13 (100%), 854.13 (58.70%), 855.13 (45.34%), 856.13 (16.99%) calcd for $C_{44}H_{32}ClP_2Pt$; found: 852.20 (89.06%), 853.22 (100%), 854.18 (58.30%), 855.29 (45.85%), 856.15 (16.81%) $[M–Cl]^+$. $[\alpha]_D^{25}$ (CH_2Cl_2): −383° (ligand: −124°).

*Synthesis of **2R***

Complex **2R** was synthesized directly from K_2PtCl_4 in DMF. Namely, 150 mg (0.36 mmol) of K_2PtCl_4 was dissolved in 10 ml of DMF at 70 °C in the dark; 102 mg of (*R*)-(+)-DABN (0.36 mmol) was added to the solution and the mixture was stirred at 40 °C in the dark overnight. The resulting yellow solution was filtrated to remove the precipitated KCl, and the solvent was then removed under reduced pressure. The crude product was precipitated with water, leading to a yellow powder that was washed with cold water, a mixture of 10:90 methanol/diethyl ether, and diethyl ether and then dried under a vacuum (yield 154 mg; 78%).

^{1}H NMR (DMF-d_7): 8.18 (2H, d, $^{3}J = 8.42$ Hz, H_{10}), 8.10 (2H, d, $^{3}J = 8.42$ Hz, H_9), 7.86 (2H, d, $^{3}J = 8.60$ Hz, H_4 or H_7), 7.52 (2H, m, H_5 or H_6), 7.47 (2H, br d, $J = 11.16$ Hz, NH_2), 7.33 (2H, m, H_5 or H_6), 6.97 (2H, d, $^{3}J = 8.60$ Hz, H_4 or H_7), 6.85 (2H, br d, $J = 11.16$ Hz, NH_2) ppm; ^{13}C{^{1}H} NMR (DMF-d_7): 139.33 (C_1), 134.03 (C_3), 132.05 (C_8), 130.37 (C_{10}), 128.59 (C_9), 126.88 (C_5 or C_6), 125.64 (C_4 or C_7), 125.29 (C_5 or C_6), 121.93 (C_2), 121.46 (C_4 or C_7) ppm; ^{195}Pt NMR (DMF-d_7): −1,866 ppm. ESI–MS (0.1:99.9 DMF/methanol): 514.06 (93.20%), 515.06 (100%), 516.06 (45.03%), 517.06 (42.19%), 518.07 (8.75%) calcd for $C_{20}H_{16}ClN_2Pt$; found: 514.48 (92.02%), 515.33 (100%), 516.12 (43.92%), 517.45 (42.12%), 518.18 (9.14%) $[M–Cl]^+$. $[\alpha]_D^{25}$ (THF): +330° (ligand: +144°).

*Synthesis of **2S***

Complex **2S** was synthesized directly from K_2PtCl_4 in DMF. Namely, 137 mg (0.33 mmol) of K_2PtCl_4 was dissolved in 10 ml of DMF at 70 °C in the dark; 94 mg of (*S*)-(−)-DABN (0.33 mmol) was added to the solution and the mixture was stirred at 40 °C in the dark overnight. The resulting yellow solution was filtrated to remove the precipitated KCl, and the solvent was then removed under reduced pressure. The crude product was precipitated with water, yielding a yellow powder that was washed with cold water, a mixture of 10: 90 methanol/diethyl ether, and diethyl ether and then dried under a vacuum (yield 130 mg; 72%).

^{1}H NMR (DMF-d_7): 8.18 (2H, d, $^{3}J = 8.42$ Hz, H_{10}), 8.10 (2H, d, $^{3}J = 8.42$ Hz, H_9), 7.86 (2H, d, $^{3}J = 8.60$ Hz, H_4 or H_7), 7.52 (2H, m, H_5 or H_6), 7.47 (2H, br d, $J = 11.16$ Hz, NH_2), 7.33 (2H, m, H_5 or H_6), 6.97 (2H, d, $^{3}J = 8.60$ Hz, H_4 or H_7), 6.85 (2H, br d, $J = 11.16$ Hz, NH_2) ppm; ^{13}C{^{1}H} NMR (DMF-d_7): 139.33 (C_1), 134.03 (C_3), 132.05 (C_8), 130.37 (C_{10}), 128.59 (C_9), 126.88 (C_5 or C_6), 125.64 (C_4 or C_7), 125.29 (C_5 or C_6), 121.93 (C_2), 121.46 (C_4 or C_7) ppm; ^{195}Pt NMR (DMF-d_7):

−1,866 ppm. ESI–MS (0.1:99.9 DMF/methanol): 514.06 (93.20%), 515.06 (100%), 516.06 (45.03%), 517.06 (42.19%), 518.07 (8.75%) calcd for $C_{20}H_{16}ClN_2Pt$; found: 514.52 (92.44%), 515.12 (100%), 516.32 (44.22%), 517.24 (42.01%), 518.23 (9.25%) $[M–Cl]^+$. $[\alpha]_D^{25}$ (THF): −330° (ligand: −144°).

Cytotoxicity tests

Three human tumor cell lines were used for the present study: A2780 (ovarian carcinoma) and HCT116 (colon adenocarcinoma) were obtained from the American Type Culture Collection (Manassas, VA, USA); A2780Cp8 cells (so-called because of their ability to grow in medium containing 8 μM cisplatin) were developed by chronic exposure of the parent cisplatin-sensitive line to increasing concentrations of cisplatin, and were obtained from R. Ozols (Fox Chase Cancer Center, Philadelphia, PA, USA). A2780Cp8 cells differ from the parental cell line in a number of features that contribute to the resistant phenotype, including alterations in mismatch and nucleotide excision DNA repair systems and increased glutathione levels. The three cell lines were maintained in RPMI-1640 (Sigma, Italy) supplemented with 10% fetal calf serum (Celbio, Italy), 2 mM L-glutamine, and a 1% streptomycin/penicillin antibiotic mixture (Sigma, Italy) under standard culture conditions (95% O_2/5% CO_2 at 37 °C in a humidified atmosphere). Cell survival following exposure to platinum complexes was evaluated using the 3-(4,5-dimethylthiazol-2-yl)-2,5-diphenyltetrazolium bromide (MTT) assay, based on the reduction of MTT by living cells [38]. Briefly, 1×10^3 cells per well were plated onto 96-well sterile plates and allowed to attach and grow for 24 h. Platinum complexes were dissolved in DMSO (cisplatin and phosphane complexes) or in ethanol (DABN complexes) to obtain 10 mM stock solutions that were diluted with complete medium for cell treatment. The final range of platinum concentrations was 10–500 μM; the cosolvent concentration never exceeded 0.1%. After 3 days, MTT was added to each well (final concentration 0.4 mg mL^{-1}) and plates were incubated for 3 h at 37 °C. Cell viability was determined by measuring the absorbance ($\lambda = 570$ nm) in individual wells, using a universal microplate reader (Bio-Tek Instruments, Winooski, VT, USA). The cytotoxic effects of platinum complexes were quantitated by calculating the drug concentration inhibiting tumor cell growth by 50% (IC_{50}), based on nonlinear regression analysis of dose–response data, performed using the Calcusyn program (Biosoft, Cambridge, UK).

G-quadruplex

5′-end ^{32}P-radiolabeled $AG_3(T_2AG_3)_3$ (22AG) was mixed with 100 μM nonradiolabeled material in 50 mM $NaClO_4$ or $KClO_4$ for 5 min at 90 °C and allowed to reach room temperature in 2 h to induce the formation of the quadruplex structure. It was then incubated with 300 μM platinum complex (*cis*-$[PtCl_2(PPh_3)_2]$, **1R**, **1S**, **2R**, or **2S**). The reactions were run for 16 h at 37 °C. The platinated oligonucleotides were separated using 20% polyacrylamide denaturing gel electrophoresis and then isolated from the gels. The platination sites were determined by means of biochemical methods using 3′-exonuclease digestion [29, 30, 34]. The kinetics of platination using intramolecular competition experiments were performed with **2R** as described elsewhere [31, 39]. The products of platination at the 5′-end ^{32}P-radiolabeled 35mer containing 22AG and at the 5′-end ^{32}P-radiolabeled 13mer containing the GG sequence were quantified after separation by gel electrophoresis using a Storm 960 phosphorimager (Molecular Dynamics, Amersham Bioscience, France).

Results and discussion

Platinum complexes

Complexes **1R** and **1S** were synthesized by reacting stoichiometric quantities of $[PtCl_2(\eta^4\text{-}1,3\text{-cyclooctadiene})]$ [35] and phosphane in CH_2Cl_2 according to published procedures [36, 37]. Complexes **2R** and **2S** were obtained by directly reacting $K_2[PtCl_4]$ with the corresponding diamine [40]. All the complexes were characterized by ESI–MS, reversed-phase high-performance liquid chromatography, UV–vis spectroscopy, and multinuclear NMR spectroscopy. In particular, ^{1}H and ^{13}C NMR signals of the complexes were assigned using one- and two-dimensional homonuclear and heteronuclear techniques such as ^{1}H,^{13}C{^{1}H} distortionless enhancement by polarization transfer with a final proton pulse angle of 135°, ^{1}H–^{1}H correlation spectroscopy, ^{1}H–^{13}C heteronuclear correlation spectroscopy, and ^{1}H–^{31}P heteronuclear correlation spectroscopy.

The performance of complex **1S** as a catalyst has already been studied by Kollár et al. [41], who described its ^{1}H NMR temperature-dependent behavior. Other NMR studies on similar complexes have been reported [42–49]. Our data confirm and complement those studies. In particular, it should be noted that for complexes **1R** and **1S**, the protons on the two different phenyl rings on the same

phosphorous atom are nonequivalent, owing to the different mobility of the rings, and show signals in different areas of the ^{1}H NMR spectrum. The signals corresponding to the more rotationally rigid ring are larger and shifted to lower frequencies, owing to the almost parallel position of the naphthalene rings.

The signals associated with the exchange-broadened peaks of the less mobile ring are labeled with a prime in "Materials and methods."

Carbons belonging to different phenyl rings on the same phosphorous atoms also exhibit different signals in the ^{13}C NMR spectrum; again, the signals corresponding to the more rotationally rigid ring are larger. In particular, the signal corresponding to C_{11}' is tricky to recognize, both in the $^{13}C\{^{1}H\}$ NMR spectrum and when using two-dimensional techniques; it probably resonates in the 123–121-ppm area. The different position of the phenyl rings, which may result in different mobility, was already observed in the X-ray structure of **1R** [50].

The reactivity of the complexes under investigation was compared by studying the solvolysis reaction in DMSO by means of conductivity measurements and NMR spectroscopy. Cisplatin underwent the Cl^{-}/DMSO exchange with a $t_{1/2}$ of 2.9 h at 25 °C and 1.2 h at 37 °C. *cis*-$[PtCl_2(PPh_3)_2]$ remained stable over 72 h at both 25 and 37 °C, as did the BINAP complexes. In contrast, the DABN complexes **2R** and **2S** underwent rapid degradation when dissolved in DMSO. This was verified via ^{195}Pt NMR spectroscopy in DMSO-d_6. The unchanged complexes, **2R** and **2S**, exhibited a chemical shift of −1,840 ppm. According to the literature [51], the amine ligand, owing to its bulkiness, is rapidly released and substituted with two DMSO molecules, resulting in the *cis*-$[PtCl_2(DMSO)_2]$ species (−3,448 ppm, about 28%). A similar amount (about 23%) of the traditional Cl^{-}/DMSO exchanged complex was also detected at −3,008 ppm. Surprisingly, the most abundant species in the spectrum (about 41%) shows a signal at −2,958 ppm, corresponding to the $[PtCl_3(DMSO)]^{-}$ complex [52].

UV–vis spectroscopy and ESI–MS were used to evaluate the solution behavior of the complexes in abiological conditions (ultrapure water, or phosphate buffer pH 7.4, or 24 mM carbonate adjusted to pH 7.4) [53] over 24 h at 37 °C with 1% cosolvent (DMSO for phosphane complexes and ethanol for amine complexes).

The general trend in water with a cosolvent is approximately the same for all the complexes. In particular, 94% of *cis*-$[PtCl_2(PPh_3)_2]$, 67% of **1R** and **2R**, and 80% of **2R** and **2S** remains intact (UV–vis spectroscopy). ESI–MS confirmed the presence of the unchanged compound along with some other species, the major one being the monoaquo complex. Furthermore, **2R** and **2S** showed traces of other degradation products. Both phosphate and carbonate remarkably speed up hydrolysis and degradation reactions.

The optical rotatory power of the complexes was determined and compared with that of the corresponding ligands. Upon coordination, the rotation direction was maintained, and the angles of optical rotation increased.

Cytotoxicity tests

Table 1 shows the IC_{50} values obtained in the three cell lines following 72-h exposure to the complexes under investigation, compared with those obtained for three reference compounds, namely, cisplatin, oxaliplatin, and *cis*-$[PtCl_2(PPh_3)_2]$.

Cisplatin was the only compound tested that showed a significant difference in the antiproliferative effect between ovarian and colorectal cells and, in fact, its low efficacy against colon cancers is well known. The other compounds appear to be equally potent in ovarian cells (including their cisplatin-resistant variant) and colorectal cells. The complexes containing phosphanes (namely, **1R** and **1S**) were slightly less potent than those containing amines, but all of them had a lower resistance factor (i.e., the ratio between IC_{50} values for cisplatin-resistant A2780Cp8 and A2780 cells) in ovarian cells than cisplatin, indicating their ability to circumvent acquired cisplatin resistance.

Interaction of the platinum complexes with the G-quadruplex

22AG was folded in the G-quadruplex structure in the presence of either Na^{+} or K^{+} (Fig. 2). Among the various conformations of G-quadruplex structures described for 22AG [54], the antiparallel structure is believed to be formed in solution with both cations [30]. This structure is rather flexible because the hydrogen bonds between the four guanines of the 5′ external G-quartet can be transiently disrupted [30]. Consequently, the guanines belonging to this 5′ external G-quartet, as well as the four free adenines in the loop regions, can form platinum adducts on their N7 atoms.

The folded structure of 22AG was incubated overnight with 3 equiv of the platinum complexes. The various platination products were then separated by gel electrophoresis and isolated (Fig. 3).

The results show that the incubation of the G-quadruplex with all the platinum complexes leads to new products that migrate more slowly than unreacted 22AG on gel electrophoresis. This indicates platination of the G-quadruplex structure of 22AG. Since the migration of oligonucleotides depends on the number of platinum adducts, the more slowly migrating products contain more than one platinum complex.

The efficiency of platination (i.e., the amount of platinated products) differs between the two pairs of isomeric

Table 1 IC_{50} values for 72-h continuous treatment of three different human tumour cell lines (A2780 ovarian carcinoma and its cisplatin-resistant variant A2780Cp8, and colon adenocarcinoma HCT116) with compounds **1R**, **1S**, **2R**, and **2S** (see Fig. 1) and the reference complexes cisplatin, oxaliplatin, and *cis*-$[PtCl_2(PPh_3)_2]$

Compound	IC_{50} (μM) A2780	IC_{50} (μM) A2780Cp8	Resistance factor	IC_{50} (μM) HCT116
Cisplatin	1.15 ± 0.09	14.99 ± 0.44*	13.03	10.98 ± 1.9**
Oxaliplatin	0.63 ± 0.11	0.55 ± 0.11	0.87	0.661 ± 0.035
cis-$[PtCl_2(PPh_3)_2]$	20.98 ± 3.5	14.47 ± 2.14	0.69	21.83 ± 6.1
1R	13.82 ± 3.53	17.51 ± 0.9	1.27	16.75 ± 3.57
1S	7.77 ± 1.71	10.48 ± 0.74	1.35	10.32 ± 0.93
2R	1.36 ± 0.3	1.58 ± 0.51	1.16	0.98 ± 0.05
2S	1.15 ± 0.11	1.27 ± 0.35	1.10	1.61 ± 0.14

*$P < 0.001$ versus A2780; **$P < 0.05$ versus A2780

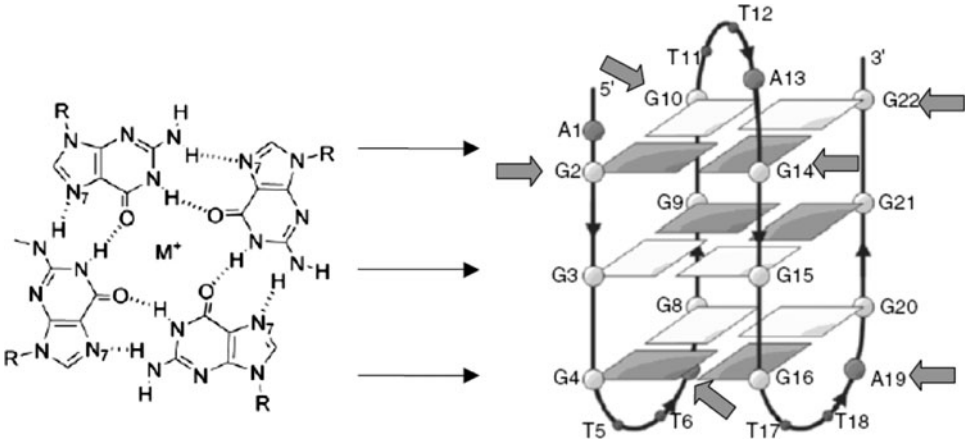

Fig. 2 Antiparallel G-quadruplex structure of 22AG (*right*) formed by the stacking of three G-quartets (*left*). The *arrows* indicate the potential platination sites

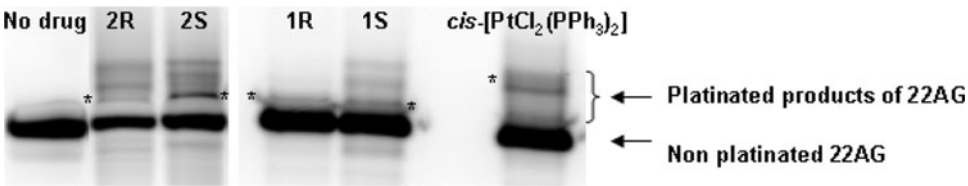

Fig. 3 Electrophoresis gel after platination of the quadruplex structure of 22AG by the platinum complexes *cis*-$[PtCl_2(PPh_3)_2]$, **1R**, **1S**, **2R**, and **2S**

complexes **1R** and **1S** and **2R** and **2S**, since the phosphane derivatives **1R** and **1S** (5 and 10%, respectively) are less reactive than the amine derivatives **2R** and **2S** (20 and 30%, respectively), likely because of the presence of two additional phenyl groups that increase the overall bulkiness of the ligands and the *trans* effect of the phosphorus atom itself. However, in both isomer pairs, the *R* isomers interact with 22AG less efficiently than their respective *S* counterparts.

Since the target DNA is a chiral macromolecule, characterized by a right-handed helical configuration [55, 56], it can differentiate between these enantiomeric alkylating agents. This assumption is confirmed in the case of oxaliplatin, namely, 1,2-diaminocyclohexane(ethanedioate-*O*,*O*)platinum(II): in fact its three possible conformational isomers [(*R*,*R*), (*S*,*S*), and (*R*,*S*), respectively] interact differently with DNA. Kidani et al. [57] showed that the (*R*,*R*) isomer was the most effective against cisplatin-sensitive and cisplatin-resistant cancer cell lines, and this is the isomer currently employed in chemotherapy [58]. Other chiral complexes show different biological activity depending on their isomeric form and affinity for DNA [59–64].

Similarly, the stereochemical arrangement of the organic ligand in these complexes plays a role in driving the interaction between the platinum moiety and nucleobases of the G-quadruplex structure of 22AG. Interestingly, although there is no direct relationship between the antiproliferative effect of alkylating agents and their ability to stabilize G-quadruplexes, the somewhat higher IC_{50} values

obtained for the *R* isomers may be associated with their lower efficiency in reacting with the target DNA.

Very recently, the first evidence that one enantiomer of a supramolecular cylinder can selectively stabilize human telomeric G-quadruplex structure was reported [65]. In particular, the *P* enantiomer has a strong preference for G-quadruplex over duplex DNA, and its selectivity has been demonstrated also by telomere shortening in cancer cells [66].

Platinum binding sites

The platinum binding sites were identified for the major platinated products (noted with an asterisk in Fig. 3) as follows:

1. *cis*-$[PtCl_2(PPh_3)_2]$ binds to A7 and A13. Since the migration of this adduct is very slow compared with that of the platination products of **1S**, **1R**, **2S**, and **2R**, it can be surmised that each 22AG molecule binds two platinum complexes, which therefore behave as monofunctional electrophilic agents.
2. **1R** and **1S** preferentially coordinate A13.
3. **2R** and **2S** are mainly bound to G10 and A19.

The platination sites identified in all the experiments are specific for platination of a G-quadruplex structure of 22AG rather than of its unfolded form, as only the adenines in the loop regions (A7, A13, or A19) and/or some guanines of the 5′ external G-quartet (G10) are readily accessible in such a structure. Moreover, the platination of G10 suggests that the antiparallel structure was trapped [29, 30]. Furthermore, when two platination sites were identified, they lay at the opposite sides of the G-quadruplex structure, indicating that the complexes under study acted as monofunctional, and not cross-linking, agents. In contrast, cisplatin was able to cross-link the G-quadruplex structure of 22AG, resulting mainly in A1–G10 and A13–G22 chelates [29]. Moreover, the bulkiest platinum complexes (**1R**, **1S**, and *cis*-$[PtCl_2(PPh_3)_2]$) platinated the same sites on the G-quadruplex structure as the two monofunctional platinum complexes containing a simple terpyridine or a *p*-tolylterpyridine [39].

The platinum binding sites depend on the nature of the ligand. In the phosphane series, platination only occurred on adenines, whereas in the amine series it also involved two guanines belonging to the 5′ external G-quartet. This difference in platination sites may be due to the bulkiness of the platinum ligands. With bulky ligands, as observed in the phosphane series, platination occurred on readily accessible platination sites, i.e., the adenines (especially A13 [30]); in contrast, amine ligands also allowed platination of some less accessible adenine or guanine residues.

Since **2R** and **2S** are able to platinate the G-quadruplex structure of the telomeric sequence, their affinity for this structure could be evaluated using melting temperature experiments. The observation of the optical density at 295 nm allows the detection of the folding and unfolding of the structure as a function of temperature. In the absence of a G-quadruplex ligand, a variation of the optical density as function of temperature that is characteristic of the folding state of the structure is observed (melting temperature of 43 °C, Fig. S2). In contrast, in the presence of **2S** or **2R**

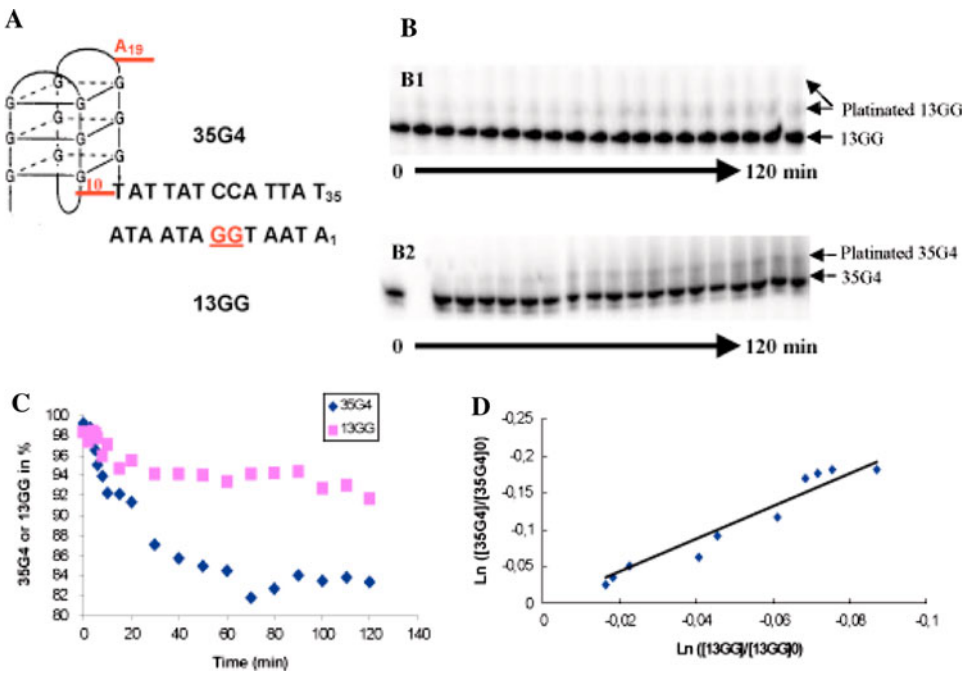

Fig. 4 **a** The 35G4/13GG system. The *underlined bases* are the platination sites for **2S**. **b** Denaturing gel electrophoresis of the kinetics of platination of the 35G4/13GG system by **2S** with radiolabeled 13GG (*B1*) or 35G4 (*B2*). **c** Concentration of the remaining 35G4 (*squares*) or 13GG (*diamonds*) as a function of time. **d** Logarithm of the ratio of the remaining amount of 35G4 as a function of the logarithm of the remaining amount of 13GG at each time point of the reaction for the determination of the rate constant ratio (k_{35G4}/k_{13GG}) of the quadruplex versus duplex DNA platination

only a slight optical density decrease was observed when increasing the temperature, suggesting that the G-quadruplex structure had been trapped, because high temperatures cannot unfold it. Therefore, it was not possible to evaluate the melting temperature of such compounds.

Affinity of the platinum complexes for the G-quadruplex structures and comparison of the kinetics of platination of double-stranded DNA and G-quadruplex structures

Since **2S** is able to platinate a G-quadruplex structure, its affinity for this structure was compared with that for duplex DNA by means of intramolecular platination competition experiments. This technique, described elsewhere [31, 39], allows comparison, in the same system, of the kinetic constants of platination of a GG site involved in a duplex DNA with a quadruplex structure. Briefly, this system consists of a 35-nucleotide DNA strand (35G4) in which the sequence of 22AG (responsible for the quadruplex component) is flanked by a 13-nucleotide tail; the duplex component is formed by the association of this tail with the complementary 13-nucleotide DNA (13GG). In the resulting system (35G4/13GG), two possible platination sites are present on each DNA architecture: G10 and A19 on the quadruplex component and G6 and G7 on the duplex component (Fig. 4).

In the case under investigation, platination of the G-quadruplex domain occurred twice as fast as platination of the double-stranded domain. This difference is of the same order of magnitude as that observed for cisplatin. Thus, replacement of the two amine groups of cisplatin by a chiral aromatic ligand does not seem to improve the selectivity of platinum complexes for G-quadruplex structures relative to that for duplex DNA.

Acknowledgments Financial support for this work was provided by the Regione Piemonte (CIPE project-code A 370 and Ricerca Sanitaria Finalizzata 2009), ATF Association (Alessandria, Italy), CNRS, and ARC 4835 (Paris, France). The study was carried out within the framework of the European Cooperation COST D39 (Metallo-Drug Design and Action) and Consorzio Interuniversitario di Ricerca in Chimica dei Metalli nei Sistemi Biologici (CIRCMSB, Bari, Italy). We are indebted to Cristina Prandi (University of Turin, Italy) for her assistance in measuring optical rotatory power.

References

1. Rosenberg B, Van Camp L, Krigas T (1965) Nature 205:698–699
2. Rosenberg B, Van Camp L, Trosko JE, Mansour VH (1969) Nature 222:385–386
3. Kelland L (2007) Nat Rev Cancer 7:573–584
4. Galanski M, Jakupec MA, Keppler BK (2005) Curr Med Chem 12:2075–2094
5. Cleare MJ, Hoeschele JD (1973) Platinum Met Rev 17:2–13
6. Cleare MJ, Hoeschele JD (1973) Bioinorg Chem 2:187–210
7. Cleare MJ (1974) Coord Chem Rev 12:349–405
8. Roundhill DM (1987) In: Wilkinson G, Gillard RD, McCleverty JA (eds) Comprehensive coordination chemistry, vol 5. Pergamon Press, Oxford, chap 52
9. Downing JH, Smith MB (2004) In: McCleverty JA, Meyer TJ (eds) Comprehensive coordination chemistry II, vol 1. Elsevier, Oxford, p 253
10. Berners-Price SJ, Sadler PJ (1988) Struct Bond 70:27–102
11. Burge S, Parkinson GN, Hazel P, Todd AK, Neidle S (2006) Nucleic Acids Res 34:5402–5415
12. Harley CB, Futcher AB, Greider CW (1990) Nature 345:458–460
13. Hiyama K, Hiyama E, Shay JW (2009) In: Hiyama K (ed) Telomeres and telomerase in cancer. Humana Press, New York, chap 1
14. Parkinson GN, Lee MPH, Neidle S (2002) Nature 417:876–880
15. Oganesian L, Bryan TM (2007) Bioessays 29:155–165
16. Parkinson EK, Minty F (2007) Biodrugs 21:375–385
17. Wong HM, Payet L, Huppert JL (2009) Curr Opin Mol Ther 11:146–155
18. De Cian A, Lacroix L, Douarre C, Temime-Smaali N, Trentesaux C, Riou JF, Mergny JL (2008) Biochimie 90:131–155
19. Villanueva JM, Jia X, Yohannes PG, Doetsch PW, Marzilli LG (1999) Inorg Chem 38:6069–6080
20. Jamieson ER, Lippard SJ (1999) Chem Rev 99:2467–2498
21. Burger AM, Double JA, Newell DR (1997) Eur J Cancer 33:638–644
22. Colangelo D, Osella D (2005) Curr Med Chem 12:3091–3102
23. Ishibashi T, Lippard SJ (1998) Proc Natl Acad Sci USA 95:4219–4223
24. Zhang G, Zhang RP, Wang XN, Xie H (2002) Cell Res 12:55–62
25. Furuta M, Nozawa K, Takemura M, Izuta S, Murate T, Tsuchiya M, Yoshida K, Taka N, Nimura Y, Yoshida S (2003) Int J Cancer 104:709–715
26. Colangelo D, Ghiglia AL, Viano I, Cavigiolio G, Osella D (2003) Biometals 16:553–560
27. Ma DL, Che CM, Yan SC (2009) J Am Chem Soc 131:1835–1846
28. Redon S, Bombard S, Elizondo-Riojas MA, Chottard JC (2001) Biochemistry 40:8463–8470
29. Redon S, Bombard S, Elizondo-Riojas MA, Chottard JC (2003) Nucleic Acids Res 31:1605–1613
30. Ourliac-Garnier I, Elizondo-Riojas MA, Redon S, Farrell NP, Bombard S (2005) Biochemistry 44:10620–10634
31. Ourliac-Garnier I, Bombard S (2007) J Inorg Biochem 101:514–524
32. Heringova P, Kasparkova J, Brabec V (2009) J Biol Inorg Chem 14:959–968
33. Monchaud D, Teulade-Fichou MP (2008) Org Biomol Chem 6:627–636
34. Bertrand H, Bombard S, Monchaud D, Teulade-Fichou MP (2007) J Biol Inorg Chem 12:1003–1014
35. Drew D, Doyle JR (1972) Inorg Synth 13:47–55
36. Ravindar V, Schumann H, Hemling H, Blum J (1995) Inorg Chim Acta 240:145–152
37. Strukul G (1997) J Mol Catal A 117:413–423
38. Alley MC, Scudiero DA, Monks A, Hursey ML, Czerwinski MJ, Fine DL, Abbott BJ, Mayo JG, Shoemaker RH, Boyd MR (1988) Cancer Res 48:589–601
39. Bertrand H, Bombard S, Monchaud D, Talbot E, Guédin A, Mergny JL, Grünert R, Bednarski PJ, Teulade-Fichou MP (2009) Org Biomol Chem 7:2864–2871
40. Miller B, Wild S, Zorbas H, Beck W (1999) Inorg Chim Acta 290:237–246
41. Kollár L, Sándor P, Szalontai G (1991) J Mol Catal 67:191–198

42. Barbaro P, Pregosin PS, Salzmann R, Albinati A, Kunz RW (1995) Organometallics 14:5160–5170
43. Pregosin PS, Trabesinger G (1998) J Chem Soc Dalton Trans 727–734
44. Nama D, Schott D, Pregosin PS, Veiros LF, Calhorda MJ (2006) Organometallics 25:4596–4604
45. Brunkan NM, Gagne MR (2002) Organometallics 21:4711–4717
46. Nama D, Pregosin PS, Albinati A, Rizzato S (2007) Organometallics 26:2111–2121
47. Pregosin PS (2008) Coord Chem Rev 252:2156–2170
48. Fuss M, Siehl HU, Olenyuk B, Stang PJ (1999) Organometallics 18:758–769
49. Fawcett J, Hope EG, Stuart AM, West AJ (2006) Polyhedron 25:1182–1186
50. Doherty S, Knight JG, Smyth CH, Harrington RW, Clegg W (2006) J Org Chem 71:9751–9764
51. Yoo J, Kim JH, Sohn YS, Do Y (1997) Inorg Chim Acta 263:53–60
52. Kerrison SJS, Sadler PJ (1985) Inorg Chim Acta 104:197–201
53. Di Pasqua AJ, Goodisman J, Kerwood DJ, Toms BB, Dubowy RL, Dabrowiak JC (2006) Chem Res Toxicol 19:139–149
54. Neidle S (2009) Curr Opin Struct Biol 19:239–250
55. Dickerson RE, Drew HR, Conner BN, Wing RM, Fratini AV, Kopka ML (1982) Science 216:475–485
56. Lerman LS, Wilkerson LS, Venable JH (1976) J Mol Biol 108:271–293
57. Kidani Y, Iigo M, Inagaki K, Hoshi A, Kuretani K (1978) J Med Chem 21:1315–1318
58. Pendyala L, Kidani Y, Perez R, Wilkes J, Bernacki RJ, Creaven PJ (1995) Cancer Lett 97:177–184
59. Benedetti M, Malina J, Kasparkova J, Brabec V, Natile G (2002) Environ Health Perspect 110:779–782
60. Vollano JF, Al-Baker S, Dabrowiak JC, Schurig JE (1987) J Med Chem 30:716–719
61. Fanizzi FP, Intini FP, Maresca L, Natile G, Quaranata R, Coluccia M, Di Bari L, Giordano D, Mariggiò MA (1987) Inorg Chim Acta 137:45–51
62. Bloemink MJ, Pérez JMJ, Heetebrij RJ, Reedijk J (1999) J Biol Inorg Chem 4:554–567
63. Malina J, Hofr C, Maresca L, Natile G, Brabec V (2000) Biophys J 78:2008–2021
64. Milanesio M, Monti E, Gariboldi MB, Gabano E, Ravera M, Osella D (2008) Inorg Chim Acta 361:2803–2814
65. Yu H, Wang X, Fu M, Ren J, Qu X (2008) Nucleic Acids Res 36:5695–5703
66. Yu H, Zhao C, Chen Y, Fu M, Ren J, Qu X (2010) J Med Chem 53:492–498